Physica A 157 (1989) 907–932
North-Holland, Amsterdam

STABILITY ANALYSIS FOR ABSORPTIVE OPTICAL BISTABILITY IN A FABRY–PÉROT CAVITY

A.J. VAN WONDEREN, B.J. DOUWES and L.G. SUTTORP
Institute for Theoretical Physics, Valckenierstraat 65, 1018 XE Amsterdam, The Netherlands

Received 3 January 1989

A stability analysis is performed for absorptive optical bistability in a medium of arbitrary absorption coefficient, which is contained in a Fabry–Pérot cavity with non-ideal mirrors. In order to describe this system we use a hierarchical set of equations which is obtained from Maxwell–Bloch theory by expanding the polarization and population inversion in slowly varying harmonics. We reduce the stability problem to two pairs of coupled differential equations for the amplitudes and the phases of the space-dependent deviations of the forward and the backward electric field envelopes. The coefficients of these equations depend on the stationary inversion fields for which a representation in terms of Chebyshev polynomials depending on the electric field envelopes is given. The influence of a truncation of the Bloch hierarchy on the instabilities is studied numerically in the uniform-field limit.

1. Introduction

Since the first experimental demonstration of the laser a wide variety of time-dependent phenomena in nonlinear optical systems has been discovered. During the last decade the theoretical understanding of these phenomena, in particular of instabilities in both active and passive devices, has greatly improved as a result of studies within the Maxwell–Bloch framework. The basis for the analytical advance in this area has been laid by Bonifacio and Lugiato, who introduced the uniform-field method [1] and furthermore excluded bidirectional light propagation [2]. The use of these simplifications in the stability analysis of the Maxwell–Bloch equations has led to analytical predictions about instabilities in both active and passive systems (for reviews see e.g. refs. [3–5]). At a later stage a closer connection with the experimental conditions has been sought, by taking into account either spatial field inhomogeneities along the longitudinal axis [6–10] or standing-wave effects [11–18]. The relevance of spatial field variations in the transverse direction has been assessed as well [19–22].

0378-4371/89/$03.50

Up to now the inclusion of standing-wave effects in the linear stability analysis of the Maxwell–Bloch equations for a nonlinear medium in a Fabry–Pérot cavity has been carried out mostly in the uniform-field limit. As this approximation is valid only if the medium is weakly coupled to the electromagnetic field and the mirrors are perfectly reflecting, the ensuing stability analysis is of limited scope. In a recent paper [23] an attempt has been made to circumvent the uniform-field limit. However, the "improved single-mode approximation" introduced in that paper effectively amounts to assuming a simple spatial dependence of the electric fields in the cavity. It is not clear whether this compromise between the exact Maxwell–Bloch equations and their uniform-field limit is sufficiently general to account for the stability behaviour of a medium with non-negligible absorption coefficient in a cavity with mirrors of finite transmission coefficient.

In the present article we shall treat the stability problem of the hierarchical set of equations which we obtain from the Maxwell–Bloch equations by expanding the polarization and the population inversion in slowly varying harmonics. This set describes a medium with a finite absorption coefficient in a Fabry–Pérot cavity with mirrors of arbitrary reflectivity. Spatial inhomogeneities in the field envelopes along the longitudinal axis will be taken into account completely. For simplicity we shall confine ourselves to the case of purely absorptive optical bistability, which implies the cooperation parameter to be non-negative and the incoming field, the cavity and the medium to be perfectly in resonance with each other.

In preparation to the linear stability analysis we shall discuss in section 2 the stationary behaviour of the Maxwell–Bloch hierarchy. It will be shown that the steady-state solutions can be represented with the help of Chebyshev polynomials of the first and the second kind. This will permit us to establish a simple connection between the slowly varying harmonics of the electric fields, the polarization and the population inversion.

The linear stability analysis is the subject of section 3. The linearized Maxwell–Bloch hierarchy with zero atomic detuning implies that the amplitude and the phase deviations of the fields evolve independently from each other. Consequently the stability problem breaks up into two separate sets of equations, which are similar in form. We shall discuss the relation of these sets with the stationary Maxwell–Bloch system and employ the latter to trace instabilities which are in resonance with the laser signal. To treat the off-resonant case we shall reduce each of the above mentioned sets to a closed system consisting of two linear differential equations for the deviations of the electric fields. For the case of a ring configuration the integration of these equations can be executed analytically; the outcome completely agrees with results derived before. For the general case of a Fabry–Pérot cavity the

solution of the differential equations is rather complicated. Recently it has been shown how it can be computed numerically [24].

The general equations obtained in the following also permit us to study the influence of truncation of the Bloch hierarchy on the stability problem. In section 4 we shall discuss this issue, returning again for convenience to the uniform-field case. In particular, we shall concentrate on the question whether higher-order truncation of the harmonic expansions for the polarization and inversion fields might lead to erroneous predictions of instabilities.

2. Stationary behaviour of the Maxwell–Bloch hierarchy

In order to describe the interaction between a classical electromagnetic field and a collection of homogeneously broadened two-level particles in a Fabry–Pérot cavity we adopt the following infinite-dimensional set of equations

$$\frac{1}{c}\frac{\partial E_{\mathrm{F}}}{\partial t}+\frac{\partial E_{\mathrm{F}}}{\partial z}=gP_{\mathrm{F},1}\,, \tag{2.1}$$

$$\frac{1}{c}\frac{\partial E_{\mathrm{B}}}{\partial t}-\frac{\partial E_{\mathrm{B}}}{\partial z}=gP_{\mathrm{B},1}\,, \tag{2.2}$$

$$\frac{\partial P_{\mathrm{F},m}}{\partial t}=-\gamma_{\perp}P_{\mathrm{F},m}+\frac{\mu}{\hbar}\left(E_{\mathrm{F}}D_{m-1}+E_{\mathrm{B}}D_{m}\right), \tag{2.3}$$

$$\frac{\partial P_{\mathrm{B},m}}{\partial t}=-\gamma_{\perp}P_{\mathrm{B},m}+\frac{\mu}{\hbar}\left(E_{\mathrm{F}}D_{m}^{*}+E_{\mathrm{B}}D_{m-1}^{*}\right), \tag{2.4}$$

$$\frac{\partial D_{0}}{\partial t}=-\gamma_{\parallel}(D_{0}+1)-\frac{2\mu}{\hbar}\left(E_{\mathrm{F}}P_{\mathrm{F},1}^{*}+E_{\mathrm{B}}P_{\mathrm{B},1}^{*}+E_{\mathrm{F}}^{*}P_{\mathrm{F},1}+E_{\mathrm{B}}^{*}P_{\mathrm{B},1}\right), \tag{2.5}$$

$$\frac{\partial D_{m}}{\partial t}=-\gamma_{\parallel}D_{m}-\frac{2\mu}{\hbar}\left(E_{\mathrm{F}}P_{\mathrm{B},m}^{*}+E_{\mathrm{B}}P_{\mathrm{B},m+1}^{*}+E_{\mathrm{F}}^{*}P_{\mathrm{F},m+1}+E_{\mathrm{B}}^{*}P_{\mathrm{F},m}\right), \tag{2.6}$$

with $m=1,2,3,\ldots$. This hierarchy of equations is obtained from the Maxwell-Bloch equations by performing a Fleck expansion [25] for the polarization, the inversion density and the electric fields, neglecting the higher harmonics of the latter [26]. The envelope fields, $\{P_{\mathrm{F},m},P_{\mathrm{B},m}\}_{m=1}^{\infty}$ for the polarization, $\{D_m\}_{m=0}^{\infty}$ for the inversion and E_{F}, E_{B} for the electric fields, are slowly varying in space (z) and time (t). The coupling constant g is equal to $\frac{1}{2}\mu nk$, where μ is the modulus of the dipole moment of the constituent paticles, k the modulus of the wave-vector of the cw laser-field, and n the particle density. The transverse and the longitudinal damping coefficients of the medium are denoted by $\gamma_{\perp}$ and $\gamma_{\parallel}$. The boundary conditions on the electric fields that are imposed by a

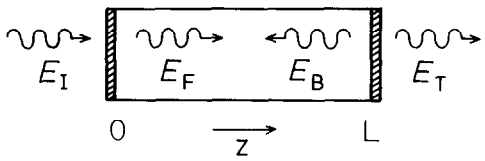

Fig. 1. Fabry–Pérot cavity with decomposition of the laser field.

Fabry–Pérot arrangement with an incident laser beam (see fig. 1) are

$$E_{\mathrm{F}}(0,t) = R^{1/2}E_{\mathrm{B}}(0,t) + T^{1/2}E_{\mathrm{I}}(t)\,, \tag{2.7}$$

$$E_{\mathrm{B}}(L,t) = R^{1/2}E_{\mathrm{F}}(L,t)\,, \tag{2.8}$$

$$E_{\mathrm{T}}(t) = T^{1/2}E_{\mathrm{F}}(L,t)\,. \tag{2.9}$$

As usual, $T = 1 - R$ stands for the transmission coefficient of the mirrors. As is clear from (2.1)–(2.9) we confine ourselves to the case of purely absorptive optical bistability, i.e. both the atoms and the cavity are assumed to be in perfect resonance with the laser frequency $\omega = ck$.

If we introduce scaled quantities

$$f = \bar{\mu}E_{\mathrm{F}}, \qquad b = \bar{\mu}E_{\mathrm{B}}\,, \tag{2.10}$$

$$y = 2\bar{\mu}T^{-1/2}E_{\mathrm{I}}, \qquad x = 2\bar{\mu}T^{-1/2}E_{\mathrm{T}}\,, \tag{2.11}$$

$$P'_{\mathrm{F},m} = (\gamma_\perp/\gamma_\parallel)^{1/2}P_{\mathrm{F},m}, \qquad P'_{\mathrm{B},m} = (\gamma_\perp/\gamma_\parallel)^{1/2}P_{\mathrm{B},m}\,, \tag{2.12}$$

with $m = 1, 2, 3, \ldots$ and $\bar{\mu} = \mu/[\hbar(\gamma_\perp\gamma_\parallel)^{1/2}]$, the coefficients in eqs. (2.1)–(2.9) get a simpler form. As a dimensionless spatial variable we introduce $\zeta = z/L$. The coupling coefficient in the Maxwell equations (2.1)–(2.2) then becomes proportional to the cooperation parameter

$$C = \frac{\mu^2 n\omega L}{2\hbar c\gamma_\perp T}\,. \tag{2.13}$$

For the case of optical bistability considered in this paper, this parameter is always positive. At a last preparatory step we truncate the Bloch hierarchy

$$P'_{\mathrm{F},m} = P'_{\mathrm{B},m} = D_m = 0, \qquad m > N\,, \tag{2.14}$$

where the truncation parameter N is a positive integer. For the following this step implies that we shall not need to operate with infinite-dimensional matrices.

In the case of a stationary incoming laser field all time derivatives may be set equal to zero. This enables one to eliminate the polarization envelope fields from the Bloch hierarchy. As a consequence the Maxwell equations can be written in terms of the inversion envelope fields $\{D_m\}$ and the electric fields f and b,

$$\frac{\mathrm{d}f}{\mathrm{d}\zeta} = CT(fD_0 + bD_1)\,, \tag{2.15}$$

$$\frac{\mathrm{d}b}{\mathrm{d}\zeta} = -CT(fD_1 + bD_0)\,, \tag{2.16}$$

while the Bloch hierarchy reduces to a matrix equation for the $(N+1)$-dimensional vector $\{D_m\}$,

$$\sum_{j=1}^{N+1} M_{(N)i,j} D_{j-1} = -\delta_{1i}\,, \tag{2.17}$$

with $i = 1, 2, 3, \ldots, N+1$. The $(N+1)\times(N+1)$ matrix $\mathbf{M}_{(N)}$ is given by

$$M_{(N)k,k} = 1 + 4f^2 + 4b^2, \qquad k = 1, 2, 3, \ldots, N\,, \tag{2.18}$$

$$M_{(N)1,2} = 8fb\,, \tag{2.19}$$

$$M_{(N)k,k+1} = 4fb, \qquad k = 2, 3, 4, \ldots, N\,, \tag{2.20}$$

$$M_{(N)k+1,k} = 4fb, \qquad k = 1, 2, 3, \ldots, N\,, \tag{2.21}$$

$$M_{(N)N+1,N+1} = 1 + 2f^2 + 2b^2\,, \tag{2.22}$$

the remaining matrix elements being zero. Eq. (2.20) is to be ignored if N equals unity. Owing to the reality of the coefficients in (2.1)–(2.9) and the free choice of the phase of the input field y all stationary fields could be taken real.

The band structure of the matrix $\mathbf{M}_{(N)}$ allows a straightforward evaluation of the stationary inversion fields

$$D_m = (-1)^{m+1}(4fb)^m \frac{|\bar{\mathbf{M}}_{(N-m)}|}{|\mathbf{M}_{(N)}|}\,, \tag{2.23}$$

with $m = 0, 1, 2, \ldots, N$. The symbol $|\mathbf{M}|$ stands for the determinant of the matrix $\mathbf{M}$. Furthermore, $\bar{\mathbf{M}}_{(N)}$ is the $N\times N$ matrix that follows from $\mathbf{M}_{(N-1)}$ by replacing its (1, 2) element by $4fb$; we define $|\bar{\mathbf{M}}_{(0)}| = 1$ and $|\bar{\mathbf{M}}_{(1)}| = 1 + 2f^2 + 2b^2$. To evaluate the right-hand side of (2.23) we consider the ratio $C_m =$

$|\bar{\mathbf{M}}_{(m)}|/(4fb)^m$. It satisfies the recurrence relation

$$C_{m+2} = 2uC_{m+1} - C_m \,, \tag{2.24}$$

for $m = 0, 1, 2, \ldots, N-2$, with the definition $u = (1 + 4f^2 + 4b^2)/(8fb)$. The solution of a recurrence relation of this type can be given in terms of continued fractions [27, 28]. Alternatively, we can write the solution of (2.24) as a linear combination of Chebyshev polynomials of the first and the second kind [29],

$$C_m = \frac{4f^2 + 4b^2}{1 + 4f^2 + 4b^2}\, T_m(u) + \frac{1}{1 + 4f^2 + 4b^2}\, U_m(u) \,, \tag{2.25}$$

with $m = 0, 1, 2, \ldots, N$. This result and the identity

$$|\mathbf{M}_{(N)}| = (1 + 4f^2 + 4b^2)|\bar{\mathbf{M}}_{(N)}| - 32f^2b^2|\bar{\mathbf{M}}_{(N-1)}| \,, \tag{2.26}$$

valid for positive integer N, can be employed to express the right-hand side of (2.23) in terms of the Chebyshev forms $\{C_m\}$,

$$D_m = \frac{(-1)^{m+1}C_{N-m}}{(1 + 4f^2 + 4b^2)C_N - 8fbC_{N-1}} \,, \tag{2.27}$$

for $m = 0, 1, 2, \ldots, N$. On substitution of the above formula in (2.3) we find for the polarization fields $\{P'_{\mathrm{F},m}\}$

$$P'_{\mathrm{F},m} = \frac{(-1)^m(fC_{N-m+1} - bC_{N-m})}{(1 + 4f^2 + 4b^2)C_N - 8fbC_{N-1}} \,, \tag{2.28}$$

with $m = 1, 2, 3, \ldots, N$. Because of the fact that the stationary Bloch set (2.3)–(2.6) is invariant for the interchange of forward (F) and backward (B) fields, we obtain the backward polarization fields from (2.28) by interchanging f and b.

Insertion of (2.27) for $m = 0, 1$ into the Maxwell equations (2.15)–(2.16) yields a closed set of differential equations for the electric fields f and b,

$$\frac{\mathrm{d}f}{\mathrm{d}\zeta} = -CT\, \frac{fC_N - bC_{N-1}}{(1 + 4f^2 + 4b^2)C_N - 8fbC_{N-1}} \,, \tag{2.29}$$

$$\frac{\mathrm{d}b}{\mathrm{d}\zeta} = CT\, \frac{bC_N - fC_{N-1}}{(1 + 4f^2 + 4b^2)C_N - 8fbC_{N-1}} \,. \tag{2.30}$$

In view of the complicated structure of the forms $\{C_N\}$ the solution of this set for arbitrary truncation parameter is troublesome; only the cases $N = 1$ and

$N = \infty$ have been treated analytically [30, 31]. However, in the uniform-field limit, corresponding to a transmission coefficient T approaching zero and a fixed cooperation parameter C, the electric fields become uniform in space and we arrive at

$$f(\zeta) = \frac{x}{2} + CTx \frac{C_N^{(\mathrm{mf})} - C_{N-1}^{(\mathrm{mf})}}{2(1+2x^2)C_N^{(\mathrm{mf})} - 4x^2 C_{N-1}^{(\mathrm{mf})}} (1-\zeta) + \mathcal{O}(T^2), \tag{2.31}$$

$$b(\zeta) = \frac{x}{2} - \frac{Tx}{4} - CTx \frac{C_N^{(\mathrm{mf})} - C_{N-1}^{(\mathrm{mf})}}{2(1+2x^2)C_N^{(\mathrm{mf})} - 4x^2 C_{N-1}^{(\mathrm{mf})}} (1-\zeta) + \mathcal{O}(T^2), \tag{2.32}$$

where we assumed analyticity of f and b for small T. The Chebyshev forms $\{C_m^{(\mathrm{mf})}\}$ are generated by the substitution of $f = b = x/2$ in the relation (2.25). From the boundary condition at $\zeta = 0$ one can explicitly evaluate now the incident amplitude y as a function of the transmitted amplitude x

$$y = x + 4Cx \frac{(u-1)(U_N - T_N)}{(u+1)U_N - T_N}, \tag{2.33}$$

with $u = 1 + 1/2x^2$ in the uniform-field limit. If we set the truncation parameter equal to infinity in the above result, we obtain the uniform-field bistability curve which arises from a complete inclusion of standing-wave effects. For increasing values of N the convergence of the function (2.33) towards this curve is slow: at $C = 20$ the coordinates $x_{(\mathrm{utp})}$ and $y_{(\mathrm{utp})}$ of the upper turning-point are given by (2.33) with a relative error smaller than one percent only if $N \geq 7$, while at $C = 210$ we must even take $N \geq 11$ in order to achieve this. The cases $N = 1$ and $N = \infty$ have been compared in [31] and [32].

For the general case of a finite mirror reflectivity we shall only consider the limit $N \to \infty$. In order to study the behaviour of the Chebyshev forms $\{C_m\}$ in this limit we use the following representation [29]:

$$C_m = \frac{4W+1}{8W} \left(\frac{1 + 4f^2 + 4b^2 + 4W}{8fb} \right)^m + \frac{4W-1}{8W} \left(\frac{1 + 4f^2 + 4b^2 - 4W}{8fb} \right)^m, \tag{2.34}$$

with $m = 0, 1, 2, \ldots$ and the definition

$$4W = [1 + 8(f^2 + b^2) + 16(f^2 - b^2)^2]^{1/2}. \tag{2.35}$$

Because of the identity

$$\frac{1+4f^2+4b^2+4W}{8fb}\cdot\frac{1+4f^2+4b^2-4W}{8fb}=1\,, \tag{2.36}$$

the first term in the right-hand side of (2.34) dominates over the second term, if m becomes large. Therefore, in the case of infinite truncation parameter the result (2.27) reads

$$D_m^{(\infty)}=-\frac{1}{4W}\left(\frac{-8fb}{1+4f^2+4b^2+4W}\right)^m\,, \tag{2.37}$$

with $m=0,1,2,\ldots$. Upon introducing the variables $\xi=f^2+b^2$ and $\psi=f^2-b^2$ we can now write the Maxwell equations (2.15)–(2.16) as

$$\frac{\mathrm{d}\xi}{\mathrm{d}\zeta}=-\frac{CT\psi}{2W}\,, \tag{2.38}$$

$$\frac{\mathrm{d}\psi}{\mathrm{d}\zeta}=CT\left(\frac{1}{8W}-\frac{1}{2}\right), \tag{2.39}$$

a result which can also be obtained by directly taking the limit $N\to\infty$ in (2.29)–(2.30). In ref. [31] this set of equations has been solved. One can verify easily that the expression $W-\xi=K$ does not depend on ζ. With the boundary condition at $\zeta=1$ this gives rise to a constraint on ξ and ψ,

$$\xi=\tfrac{1}{4}-K+[\psi^2+\tfrac{1}{8}-\tfrac{1}{2}K]^{1/2}\,, \tag{2.40}$$

where K follows from

$$4K=-x^2(1+R)+[T^2x^4+2x^2(1+R)+1]^{1/2}\,. \tag{2.41}$$

In (2.40) the sign in front of the root is determined by the inequality $\xi-\frac{1}{4}+K=W-\frac{1}{4}\geqslant 0$. The existence of the conserved quantity $W-\xi$ opens the possibility to reduce the two-dimensional set (2.38)–(2.39) to the one-dimensional differential equation

$$-CT\,\mathrm{d}\zeta=2\,\mathrm{d}\psi+2(16\psi^2+2-8K)^{-1/2}\,\mathrm{d}\psi\,, \tag{2.42}$$

and so to obtain after integration and fitting of the boundary condition at $\zeta=1$

$$[\psi+(\psi^2+\tfrac{1}{8}-\tfrac{1}{2}K)^{1/2}]\exp(4\psi)=(K-\tfrac{1}{4}+\tfrac{1}{2}x^2)\exp[2CT(1-\zeta)+Tx^2]\,. \tag{2.43}$$

The left-hand side is a monotonously increasing function of ψ. Hence for fixed x this relation determines ψ uniquely for each ζ. The solution satisfies the inequalities

$$\tfrac{1}{4}Tx^2 \leqslant \psi \leqslant \tfrac{1}{4}Tx^2 + \tfrac{1}{2}CT(1-\zeta)\,. \tag{2.44}$$

We now can calculate from (2.40) and (2.43), at least numerically, the fields f and b as a function of ζ for arbitrary values of C, T and x. Therefore the steady-state behaviour of the set (2.1)–(2.6) with the boundary conditions (2.7)–(2.9) is completely known.

3. Linear stability analysis of the Maxwell–Bloch hierarchy

The stability of the steady-state solutions discussed in the previous section is investigated in the usual way, namely by substituting for all envelope fields in the Maxwell–Bloch hierarchy the stationary expressions augmented by a small time-dependent deviation. After linearization the equations decouple into two separate sets: one set for the amplitude deviations

$$\Delta^{(+)}v(\zeta,t) = \delta|v(\zeta,t)| = \tfrac{1}{2}[\delta v(\zeta,t) + \delta v(\zeta,t)^*]\,, \tag{3.1}$$

and another for the phase deviations

$$\Delta^{(-)}v(\zeta,t) = \mathrm{i}v^{\mathrm{st}}(\zeta)\delta[\arg v(\zeta,t)] = \tfrac{1}{2}[\delta v(\zeta,t) - \delta v(\zeta,t)^*]\,, \tag{3.2}$$

for any envelope field v. These sets have the form

$$\frac{\partial}{\partial t}\Delta^{(\pm)}\tilde{\boldsymbol{x}}(\zeta,t) = \mathbf{L}^{(\pm)}(\zeta)\cdot\Delta^{(\pm)}\tilde{\boldsymbol{x}}(\zeta,t)\,. \tag{3.3}$$

Here $\mathbf{L}^{(+)}$ and $\mathbf{L}^{(-)}$ are linear operators which map a real orginal onto a real image. The real deviation vector $\Delta^{(+)}\tilde{\boldsymbol{x}}(\zeta,t)$ is a $(3N+3)$-dimensional column vector made up of the amplitude deviations of all the envelope fields. On the other hand the imaginary column vector $\Delta^{(-)}\tilde{\boldsymbol{x}}(\zeta,t)$, which determines the phase deviations, has only $3N+2$ components, since the inversion field envelope D_0 is real. The solution of the above sets of equations can be written down formally as

$$\Delta^{(\pm)}\tilde{\boldsymbol{x}}(\zeta,t) = \sum_l c_l \Delta^{(\pm)}\boldsymbol{x}_l(\zeta)\exp(\lambda_l^{(\pm)}t)\,, \tag{3.4}$$

with $\Delta^{(\pm)}\boldsymbol{x}_l$ and $\lambda_l^{(\pm)}$ an eigenvector of the operator $\mathbf{L}^{(\pm)}$ and its corresponding

eigenvalue, so that one has

$$\mathbf{L}^{(\pm)}(\zeta)\cdot\Delta^{(\pm)}\boldsymbol{x}_l(\zeta)=\lambda_l^{(\pm)}\Delta^{(\pm)}\boldsymbol{x}_l(\zeta)\,. \tag{3.5}$$

Because of the fact that this equation is equally true if we replace $\Delta^{(\pm)}\boldsymbol{x}_l$ and $\lambda_l^{(\pm)}$ by their complex conjugates, the linear combination at the right-hand side of (3.4) can be chosen such that the sum is real or imaginary, in accordance with the definitions (3.1) and (3.2).

In order to analyze the stability of the solutions of (3.3) we replace $\Delta^{(\pm)}\tilde{\boldsymbol{x}}(\zeta,t)$ by $\Delta^{(\pm)}\boldsymbol{x}(\zeta)\exp(\lambda t)$, solve for the eigenvalue and check the sign of its real part. The two sets of equations that are generated from the Maxwell–Bloch set (2.1)–(2.6) with (2.10)–(2.12) by this procedure are

$$\frac{\mathrm{d}\Delta^{(\pm)}f}{\mathrm{d}\zeta}=-\tilde{\lambda}\Delta^{(\pm)}f+CT\Delta^{(\pm)}P'_{\mathrm{F},1}\,, \tag{3.6}$$

$$-\frac{\mathrm{d}\Delta^{(\pm)}b}{\mathrm{d}\zeta}=-\tilde{\lambda}\Delta^{(\pm)}b+CT\Delta^{(\pm)}P'_{\mathrm{B},1}\,, \tag{3.7}$$

$$\lambda_\perp\Delta^{(\pm)}P'_{\mathrm{F},m}=f\Delta^{(\pm)}D_{m-1}+D_{m-1}\Delta^{(\pm)}f+b\Delta^{(\pm)}D_m+D_m\Delta^{(\pm)}b\,, \tag{3.8}$$

$$\lambda_\perp\Delta^{(\pm)}P'_{\mathrm{B},m}=\pm f\Delta^{(\pm)}D_m+D_m\Delta^{(\pm)}f\pm b\Delta^{(\pm)}D_{m-1}+D_{m-1}\Delta^{(\pm)}b\,, \tag{3.9}$$

$$-\tfrac{1}{2}\lambda_\parallel\Delta^{(+)}D_0=2f\Delta^{(+)}P'_{\mathrm{F},1}+2P'_{\mathrm{F},1}\Delta^{(+)}f+2b\Delta^{(+)}P'_{\mathrm{B},1}+2P'_{\mathrm{B},1}\Delta^{(+)}b\,, \tag{3.10}$$

$$\begin{aligned}-\tfrac{1}{2}\lambda_\parallel\Delta^{(-)}D_m=&f\Delta^{(-)}P'_{\mathrm{F},m+1}\pm P'_{\mathrm{F},m+1}\Delta^{(-)}f+b\Delta^{(-)}P'_{\mathrm{F},m}\pm P'_{\mathrm{F},m}\Delta^{(-)}b\\&\pm f\Delta^{(-)}P'_{\mathrm{B},m}+P'_{\mathrm{B},m}\Delta^{(-)}f\pm b\Delta^{(-)}P'_{\mathrm{B},m+1}+P'_{\mathrm{B},m+1}\Delta^{(-)}b\,,\end{aligned} \tag{3.11}$$

with $m=1,2,3,\ldots,N$ and with the definitions $\tilde{\lambda}=\lambda Lc^{-1}$ and $\lambda_i=1+\gamma_i^{-1}\lambda$ for $i=\perp,\parallel$. The coefficients in front of the deviations at the right-hand sides of (3.8)–(3.11) are the stationary envelopes discussed in the previous section. Truncation has been introduced again by stipulating (2.14) both for the deviations and for the stationary fields. The deviations of the electric fields obey a pair of boundary conditions,

$$\Delta^{(\pm)}f(0)=R^{1/2}\Delta^{(\pm)}b(0)\,, \tag{3.12}$$

$$\Delta^{(\pm)}f(1)=R^{-1/2}\Delta^{(\pm)}b(1)\,. \tag{3.13}$$

The input field y has been kept at its stationary value, since we wish to describe intrinsic instabilities only.

The set of equations (3.6)–(3.11), together with the boundary condition (3.13) and the equality $\Delta^{(\pm)}f(1) = \Delta^{(\pm)}x/2$, uniquely determines the deviations $\Delta^{(\pm)}f(\zeta)$ and $\Delta^{(\pm)}b(\zeta)$ for any value of $\tilde{\lambda}$. The condition (3.12) serves as an additional constraint which is needed to solve the stability problem. In general, the result for the eigenvalue $\tilde{\lambda}$ will be complex. However, if we take $\mathrm{Im}\,\tilde{\lambda} = 0$ the coefficients of eqs. (3.6)–(3.11) become real and, as a consequence, the solutions for the deviations $\Delta^{(\pm)}f(0)$ and $\Delta^{(\pm)}b(0)$ are real as well. Then the freedom in the choice of $\mathrm{Re}\,\tilde{\lambda}$ can be used to try and meet the requirement (3.12); it should be noted that the existence of a solution for $\mathrm{Re}\,\tilde{\lambda}$ is not a priori obvious, since the eigenvalue problem is nonlinear. Instabilities which are found upon assuming $\mathrm{Im}\,\tilde{\lambda} = 0$ are generated by the cavity mode that oscillates at the same frequency as the laser signal. As we shall demonstrate now, information on these resonant instabilities can be acquired by employing the stationary theory, discussed in the previous section.

If we add small increments to the amplitudes and the phases of the stationary fields and derive equations for these increments with the help of the stationary Maxwell–Bloch theory, the equations (3.6)–(3.11) are recovered, with $\tilde{\lambda}$ set equal to zero; the condition (3.13) is found as well. This means that for $\tilde{\lambda} = 0$ the deviations $\Delta^{(\pm)}f(\zeta)$ and $\Delta^{(\pm)}b(\zeta)$ of the electric fields are completely determined by stationary theory. As a consequence we may derive a constraint on these deviations for $\zeta = 0$. From a comparison with the condition (3.12) one learns then whether circumstances exist under which $\tilde{\lambda} = 0$ is the solution of the stability problem or, said differently, under which the character of the resonant mode changes from stable to unstable. Firstly focusing on the amplitude instabilities, we can find a constraint on the deviations $\Delta^{(+)}f(0)$ and $\Delta^{(+)}b(0)$ from the boundary condition (2.7). If we write down this condition for small increments of the electric fields and use $\Delta^{(+)}y = (\mathrm{d}y/\mathrm{d}x)\Delta^{(+)}x$, the result reads

$$\Delta^{(+)}f(0) - R^{1/2}\Delta^{(+)}b(0) = T\,\frac{\mathrm{d}y}{\mathrm{d}x}\,\Delta^{(+)}f(1)\,. \tag{3.14}$$

Thus we may conclude that for $\tilde{\lambda} = 0$ the condition (3.12), with the plus sign, is matched only if the output amplitude x is chosen such that a turning point of the steady-state curve $y(x)$ is attained. Hence, solely at these points of the bistability curve the resonant mode becomes unstable against amplitude perturbations.

As to the resonant phase instabilities, one can prove easily that the phases of the stationary electric fields equal the phase of the stationary input field, which implies

$$\frac{\Delta^{(-)}f(0)}{\Delta^{(-)}b(0)} = \frac{f(0)}{b(0)}\,, \tag{3.15}$$

if $\tilde{\lambda}$ equals zero. From the inequality $f(0) > b(0)$ it is manifest that the condition (3.12) can never be satisfied. We have shown now in a formal way that resonant amplitude instabilities are present only in the negative-slope part of the steady-state curve, whereas resonant phase instabilities do not occur. Of course, in order to study the instabilities which generate off-resonant oscillations one has to solve the linearized Maxwell–Bloch hierarchy explicitly.

In solving the off-resonant stability problem the first step is the calculation of $\Delta^{(\pm)}P'_{\mathrm{F},1}$ and $\Delta^{(\pm)}P'_{\mathrm{B},1}$ from the Bloch-type equations (3.8)–(3.11) in terms of the stationary fields and the variations of the electric fields, so that the differential equations (3.6)–(3.7) become a closed system. Concentrating first on the set for the amplitude deviations we eliminate all polarization fields from (3.8)–(3.11) and obtain in this way a matrix equation for the $(N+1)$-dimensional vector $\{\Delta^{(+)}D_{j-1}\}$

$$\lambda_{\mathrm{p}} \sum_{j=1}^{N+1} M_{(\lambda,N)i,j}\Delta^{(+)}D_{j-1} = -F_i^{(+)}\Delta^{(+)}f - B_i^{(+)}\Delta^{(+)}b\,, \tag{3.16}$$

with $i = 1, 2, 3, \ldots, N+1$ and $\lambda_{\mathrm{p}} = \lambda_{\perp}\lambda_{\parallel}$. The $(N+1)\times(N+1)$ matrix $\mathbf{M}_{(\lambda,N)}$ is generated from the matrix $\mathbf{M}_{(N)}$, defined by (2.18)–(2.22), by the substitutions

$$f \rightarrow f_{\lambda} = \lambda_{\mathrm{p}}^{-1/2} f\,, \tag{3.17}$$

$$b \rightarrow b_{\lambda} = \lambda_{\mathrm{p}}^{-1/2} b\,. \tag{3.18}$$

The $N+1$ elements of the column vector $\boldsymbol{F}^{(+)}$ are defined by the following combinations of stationary fields:

$$F_1^{(+)} = 4(1+\lambda_{\perp})(fD_0 + bD_1)\,, \tag{3.19}$$

$$F_i^{(+)} = 2(1+\lambda_{\perp})(2fD_{i-1} + bD_{i-2} + bD_i)\,, \tag{3.20}$$

$$F_{N+1}^{(+)} = 2(1+\lambda_{\perp})(fD_N + bD_{N-1})\,, \tag{3.21}$$

with $i = 2, 3, 4, \ldots, N$. The interchange of f and b transforms the column vectors $\boldsymbol{F}^{(+)}$ and $\boldsymbol{B}^{(+)}$ into each other.

As can be seen from (3.8)–(3.9) only the deviations $\Delta^{(+)}D_0$ and $\Delta^{(+)}D_1$ have to be determined. The elements of the inverse matrix that are needed are found along the same lines as in section 2; they read

$$[\mathbf{M}^{-1}_{(\lambda,N)}]_{11} = -D_{\lambda,0}, \qquad [\mathbf{M}^{-1}_{(\lambda,N)}]_{1j} = -2D_{\lambda,j-1}\,, \tag{3.22}$$

$$[\mathbf{M}^{-1}_{(\lambda,N)}]_{21} = -D_{\lambda,1}, \qquad [\mathbf{M}^{-1}_{(\lambda,N)}]_{2j} = \frac{1+4f_{\lambda}^2+4b_{\lambda}^2}{4f_{\lambda}b_{\lambda}}\, D_{\lambda,j-1}\,, \tag{3.23}$$

with $j = 2, 3, 4, \ldots, N+1$. The subscript λ indicates that the substitutions (3.17)–(3.18) must be performed throughout. We now can carry out the task of eliminating the polarization deviations from (3.6)–(3.7). After some technical manipulations, discussed in the Appendix, we find the following set of coupled linear differential equations for the amplitude deviations of the electric field envelopes:

$$\frac{\mathrm{d}}{\mathrm{d}\zeta}\begin{pmatrix}\Delta^{(+)}f\\ \Delta^{(+)}b\end{pmatrix}=\begin{pmatrix}H_{11}^{(+)} & H_{12}^{(+)}\\ H_{21}^{(+)} & H_{22}^{(+)}\end{pmatrix}\begin{pmatrix}\Delta^{(+)}f\\ \Delta^{(+)}b\end{pmatrix}. \tag{3.24}$$

The matrix elements in the first line are given by

$$\begin{aligned}H_{11}^{(+)} = &-\tilde{\lambda} + CT\,\frac{1+\lambda_\perp^{-1}}{16f^2}\left[1+\frac{(1-4f^2+4b^2)^2}{1-\lambda_\mathrm{p}}\,D_0\right.\\ &\left.+\frac{(1-4f_\lambda^2+4b_\lambda^2)^2}{1-\lambda_\mathrm{p}^{-1}}\,D_{\lambda,0}+4(1-4f_\lambda^2+4b_\lambda^2)(f^2-b^2)D_N D_{\lambda,N}\right]\\ &+CT\lambda_\perp^{-1}D_0\,,\end{aligned} \tag{3.25}$$

$$\begin{aligned}H_{12}^{(+)} = CT\,\frac{1+\lambda_\perp^{-1}}{16fb}&\left[1+\frac{1-(4f^2-4b^2)^2}{1-\lambda_\mathrm{p}}\,D_0+\frac{1-(4f_\lambda^2-4b_\lambda^2)^2}{1-\lambda_\mathrm{p}^{-1}}\,D_{\lambda,0}\right.\\ &\left.-4(1-4f_\lambda^2+4b_\lambda^2)(f^2-b^2)D_N D_{\lambda,N}\right]+CT\lambda_\perp^{-1}D_1\,.\end{aligned} \tag{3.26}$$

The other two elements follow from the symmetry relations

$$H_{21}^{(+)}(f,b) = -H_{12}^{(+)}(b,f)\,, \tag{3.27}$$

$$H_{22}^{(+)}(f,b) = -H_{11}^{(+)}(b,f)\,. \tag{3.28}$$

In the appendix it is demonstrated that the set governing the phase deviations can be transformed to the form (3.24) as well. The matrix elements $H_{ij}^{(-)}$ satisfy symmetry relations analogous to (3.27)–(3.28). Hence, they are completely determined by the formulas

$$\begin{aligned}H_{11}^{(-)} = &-\tilde{\lambda} + CT\,\frac{(1+\lambda_\perp^{-1})}{16f^2}\,G+\frac{1}{2}\,CT(1-\lambda_\perp^{-1})D_N D_{\lambda,N}D_{\lambda,0}^{-1}\\ &+CT\lambda_\perp^{-1}D_0\,,\end{aligned} \tag{3.29}$$

$$\begin{aligned}H_{12}^{(-)} = &-CT\,\frac{(1+\lambda_\perp^{-1})}{16fb}\,G-\frac{1}{2}\,CT(1-\lambda_\perp^{-1})\,\frac{b}{f}\,D_N D_{\lambda,N}D_{\lambda,0}^{-1}\\ &+CT\lambda_\perp^{-1}D_1\,,\end{aligned} \tag{3.30}$$

with the quantity G defined by

$$G = -1 + \frac{16W^2 D_0}{\lambda_p - 1} + \frac{D_{\lambda,0}^{-1}}{\lambda_p^{-1} - 1} + \frac{4(1+\lambda_p)(f^2+b^2) + 16(f^2-b^2)^2}{1-\lambda_p} D_N D_{\lambda,N} D_{\lambda,0}^{-1}. \tag{3.31}$$

So far we have dealt with the linear stability analysis for the truncated Maxwell–Bloch hierarchy. Thus the matrix elements $H_{ij}^{(\pm)}$, as given by (3.25)–(3.31), depend on the truncation parameter N. If we want to include standing-wave effects completely, we have to take the limit $N \to \infty$ of these matrix elements. We then need the limiting expressions of the inversion fields $\{D_m\}$ and $\{D_{\lambda,m}\}$ for $m = 0, 1$. Furthermore, we have to consider D_N and $D_{\lambda,N}$ for $N \to \infty$.

The inversion fields D_0 and D_1 for large truncation parameter follow directly from (2.37). From these the expressions for $D_{\lambda,0}$ and $D_{\lambda,1}$ are obtained by the replacements $f \to f_\lambda$ and $b \to b_\lambda$. The square root W, defined in (2.35), then transforms into the complex square root W_λ. The prescription for the sign of this square root can be determined by returning to (2.34), with f_λ and b_λ inserted. For large m the first term is dominant, if the sign of W_λ is chosen in accordance with

$$\mathrm{Re}\, \frac{W_\lambda}{1 + 4f_\lambda^2 + 4b_\lambda^2} > 0. \tag{3.32}$$

If the value of λ is such that the ratio of the forms at the left-hand side is purely imaginary or that one of these forms vanishes, both terms in (2.34) contribute for large m, so that in that case the limiting expressions for $\{D_{\lambda,m}\}$ become more complicated. However, this situation does not occur if the real part of the eigenvalue λ is non-negative.

The inversion fields D_N and $D_{\lambda,N}$ can be neglected in the limit $N \to \infty$. This follows from (2.27), since according to (2.34) the moduli of the Chebyshev forms C_N and $C_{\lambda,N}$ increase beyond bounds if N tends to ∞. The evaluation of the matrix elements $H_{ij}^{(\pm)(\infty)}$ is thus only a matter of substituting the expressions for the inversion fields $D_{\lambda,0}^{(\infty)}$, $D_0^{(\infty)}$ and $D_1^{(\infty)}$ in (3.25)–(3.31). The results can be verified by calculating the matrices $\mathbf{H}^{(\pm)(\infty)}$ from the linearized Maxwell–Bloch equations for the complete polarization and inversion fields, without using the Fleck expansion. For the uniform-field case this method has been employed in ref. [15].

Incidentally, it may be remarked that one can derive the stability properties for a ring cavity as well in the present context. To this end we let the stationary

backward electric field approach zero. Then we may write

$$4W = 1 + 4f^2 + 4b^2 \frac{1 - 4f^2}{1 + 4f^2} + \mathcal{O}(b^4) . \tag{3.33}$$

Insertion of this relation into the formulas (3.26) and (3.30) for $N \to \infty$ gives immediately that the matrix elements $H_{12}^{(\pm)(\infty)}$ vanish if b becomes small. This implies that the deviations of the forward and the backward electric field are no longer coupled to each other; the sets which describe the amplitude and phase deviations both split up into a pair of linear differential equations. These can be obtained explicitly by entering the result (3.33) into the expressions (3.25) and (3.29), with $N = \infty$, for the matrix elements $H_{ii}^{(\pm)(\infty)}$. As a result of the above steps the system (3.24) reduces to a set of equations which has been found previously [2, 13]. The amplitude deviation of the forward electric field satisfies

$$\frac{\mathrm{d}}{\mathrm{d}\zeta} \Delta^{(+)} f = -\tilde{\lambda} \Delta^{(+)} f + CT \frac{4f_\lambda^2 - \lambda_\perp^{-1}}{(1 + 4f^2)(1 + 4f_\lambda^2)} \Delta^{(+)} f . \tag{3.34}$$

Integration of this equation can be performed with the help of the stationary relation (2.38), which reads now

$$\frac{\mathrm{d}f}{\mathrm{d}\zeta} = -\frac{CTf}{1 + 4f^2} . \tag{3.35}$$

To fix the constant of integration we impose the well-known boundary condition for a ring cavity [2, 3]

$$\Delta^{(\pm)} f(0) = R \Delta^{(\pm)} f(1) \exp[\lambda c^{-1} (L - \mathscr{L})] , \tag{3.36}$$

with $\mathscr{L}$ the cavity round-trip length, and accordingly find the eigenvalue λ as

$$\frac{\lambda_{\mathrm{F}}^{(+)} \mathscr{L}}{c} = 2\pi n \mathrm{i} + \log R - \frac{1}{2} (1 + \lambda_\perp^{-1}) \log\left(\frac{1 + 4f_\lambda^2(1)}{1 + 4f_\lambda^2(0)} \right) + \lambda_\perp^{-1} \log\left(\frac{f(1)}{f(0)} \right) . \tag{3.37}$$

Here we must substitute

$$f(0) = \tfrac{1}{2} Rx + \tfrac{1}{2} Ty, \qquad f(1) = \tfrac{1}{2} x . \tag{3.38}$$

The spectrum of instabilities, generated by (3.37), has been the subject of many studies during the last decade [2, 6, 8, 9, 33]. Integration of the

differential equation for the phase deviation of the forward electric field yields with the help of (3.36)

$$\frac{\lambda_F^{(-)}\mathscr{L}}{c} = 2\pi n\mathrm{i} + \log R + \lambda_\perp^{-1} \log\left(\frac{f(1)}{f(0)}\right). \tag{3.39}$$

The real part of the right-hand side is always negative. The remaining differential equations for the deviations of the backward electric field are quite analogous. Integration can be performed in a similar way as shown above. After application of the boundary conditions

$$\Delta^{(\pm)}b(0) = R^{-1}\Delta^{(\pm)}b(1)\exp[\lambda c^{-1}(\mathscr{L} - L)], \tag{3.40}$$

the outcome is

$$\frac{\lambda_B^{(\pm)}\mathscr{L}}{c} = 2\pi n\mathrm{i} + \log R - \frac{1}{4}(1 + \lambda_\perp^{-1}) \log\left(\frac{1 + 4f_\lambda^2(1)}{1 + 4f_\lambda^2(0)}\right) + \lambda_\perp^{-1} \log\left(\frac{f(1)}{f(0)}\right). \tag{3.41}$$

For a ring configuration amplitude and phase instabilities in the backward propagating fields are governed by the same equation.

Returning to the Fabry–Pérot case, we state as a conclusion of the present treatment that the linear stability analysis of the Maxwell–Bloch hierarchy (2.1)–(2.6) can be formulated in terms of two sets of linear differential equations, one describing the amplitude deviations and the other the phase deviations. The coefficients figuring in these sets have been expressed in the stationary electric fields f and b. Altogether, we have paved the way to investigate side-mode instabilities for absorptive optical bistability in a non-ideal standing-wave cavity [24, 34]. It should be mentioned here that the application of our results is not exclusively restricted to this area. The stability properties of an active medium can be investigated along the same lines, since this case differs from that of a passive medium only by the sign of the cooperation parameter C.

As a final topic of this paper we will discuss the dependence of the amplitude instabilities on the value of the truncation parameter N. This discussion will be limited to the uniform-field case only. As a starting point we shall adopt the set of equations (3.24) with (3.25)–(3.26), supplemented by the boundary conditions (3.12)–(3.13). The results will be compared with those found previously [11, 14–16]. In a future publication [34] a similar discussion will be presented for phase instabilities.

4. Influence of truncation on amplitude instabilities in the uniform-field case

From now on we confine ourselves to the uniform-field limit, since in that case a further analytical treatment of the instability problem for the Fabry–Pérot cavity can be given. Moreover, a direct comparison with previous work will be possible in this way. Upon expansion of $\tilde{\lambda}$ in powers of T and insertion of the form $x/2 + \mathcal{O}(T)$ for f and b, in accordance with (2.31)–(2.32), the differential equations (3.24) become

$$\frac{\mathrm{d}}{\mathrm{d}\zeta}\begin{pmatrix}\Delta^{(+)}f\\ \Delta^{(+)}b\end{pmatrix} = (\tilde{\lambda}^{(0)} + T\tilde{\lambda}^{(1)})\begin{pmatrix}-1 & 0\\ 0 & 1\end{pmatrix}\begin{pmatrix}\Delta^{(+)}f\\ \Delta^{(+)}b\end{pmatrix} + CT\begin{pmatrix}A^{(+)} & B^{(+)}\\ -B^{(+)} & -A^{(+)}\end{pmatrix}\begin{pmatrix}\Delta^{(+)}f\\ \Delta^{(+)}b\end{pmatrix} + \mathcal{O}(T^2)\,. \tag{4.1}$$

The boundary conditions read up to first order in T

$$\Delta^{(+)}f(0) = (1 - \tfrac{1}{2}T)\Delta^{(+)}b(0), \qquad \Delta^{(+)}f(1) = (1 + \tfrac{1}{2}T)\Delta^{(+)}b(1)\,. \tag{4.2}$$

The matrix element $A^{(+)}$ in (4.1) is equal to

$$A^{(+)} = \frac{1 + \lambda_\perp^{-1}}{4x^2}\left(1 + \frac{D_0^{(\mathrm{mf})}}{1 - \lambda_\mathrm{p}} + \frac{D_{\lambda,0}^{(\mathrm{mf})}}{1 - \lambda_\mathrm{p}^{-1}}\right) + \lambda_\perp^{-1} D_0^{(\mathrm{mf})}\,. \tag{4.3}$$

Here $D_0^{(\mathrm{mf})}$ is obtained from D_0 by the substitution $f = b = x/2$. The matrix element $B^{(+)}$ differs from $A^{(+)}$ only in the last term of (4.3) which is to be replaced by $\lambda_\perp^{-1} D_1^{(\mathrm{mf})}$.

In lowest order of T the eigenvalue $\tilde{\lambda}^{(0)}$ equals $\pi n\mathrm{i}$, with integer n. The first-order contribution to the resonant mode, for which n is zero, can be determined from

$$\tilde{\lambda}_0^{(1)} = -\tfrac{1}{2} + CA^{(+)}(\lambda \to 0) + CB^{(+)}(\lambda \to 0)\,. \tag{4.4}$$

Evaluation of the right-hand side of this equation leads to

$$\tilde{\lambda}_0^{(1)} = -\frac{1}{2} + C\left(\frac{1}{2x^2} + \frac{D_0^{(\mathrm{mf})}}{2x^2} - \frac{1}{2x}\frac{\mathrm{d}}{\mathrm{d}x} D_0^{(\mathrm{mf})}\right). \tag{4.5}$$

If we solve (2.15)–(2.16) with the boundary conditions (2.7)–(2.9) in the uniform-field limit and use (A.2) we arrive at

$$y = x + \frac{C}{x}\,(1 + D_0^{(\mathrm{mf})})\,, \tag{4.6}$$

an equality which can also be obtained directly from (2.33) with (2.27). Differentiation of the right-hand side yields with (4.5)

$$\tilde{\lambda}_0^{(1)} = -\frac{1}{2}\frac{\mathrm{d}y}{\mathrm{d}x} . \tag{4.7}$$

For $N = 1$ and $N = \infty$ this result corroborates earlier work [11, 15, 16].

Turning to the side modes, with $\tilde{\lambda}_n^{(0)} = \pi n \mathrm{i}$, we note that the first-order eigenvalue $\tilde{\lambda}_n^{(1)}$ does not contain the term with $B^{(+)}$ and consequently (4.3) implies

$$\tilde{\lambda}_n^{(1)} = -\frac{1}{2} + C\frac{1+\lambda_\perp^{-1}}{4x^2}\left(1 + \frac{D_0^{(\mathrm{mf})}}{1-\lambda_\mathrm{p}} + \frac{D_{\lambda,0}^{(\mathrm{mf})}}{1-\lambda_\mathrm{p}^{-1}}\right) + C\lambda_\perp^{-1} D_0^{(\mathrm{mf})} , \tag{4.8}$$

where for λ_j we should insert $1 + \mathrm{i}\pi\tau_j$, with $\tau_j = nc/L\gamma_j$, for non-vanishing integer n and $j = \perp, \|$. The physical case, corresponding to $N = \infty$, can be derived from (4.8), if we employ the formula (2.37) for $m = 0$, from which the equality $D_0^{(\mathrm{mf})(\infty)} = -(1+4x^2)^{-1/2}$ may be inferred. After entering this result in (4.8) we find [15, 16]

$$\tilde{\lambda}_n^{(1)(\infty)} = -\frac{1}{2} + C\frac{1+\lambda_\perp^{-1}}{4x^2}\left(1 + \frac{U^{-1}}{\lambda_\mathrm{p}-1} + \frac{U_\lambda^{-1}}{\lambda_\mathrm{p}^{-1}-1}\right) - C\lambda_\perp^{-1}U^{-1} . \tag{4.9}$$

Here we defined $U = (1+4x^2)^{1/2}$ and $U_\lambda = (1+4\lambda_\mathrm{p}^{-1}x^2)^{1/2}$ with $\mathrm{Re}\, U_\lambda > 0$. Furthermore, if N is set equal to unity in (4.8), the result of ref. [11] is recovered.

A suitable way to determine the location of the side-mode amplitude instabilities, described by (4.8), as a function of the physical parameters consists in scanning the boundaries of the instability domain in the $(x, \tau_\perp)$-plane. This can be achieved by solving numerically the equation

$$\mathrm{Re}\, \tilde{\lambda}_n^{(1)}[x, \tau_\perp, C, N, d] = 0 , \tag{4.10}$$

with $d = \gamma_\| / \gamma_\perp$. As an example we show the result for $C = 210$, $d = 1$ and $N = 1, 2, 5, \infty$ in fig. 2. Clearly the shape of the instability domain sensitively depends on the value of the truncation parameter N. For $N = 2$ the instability domain even breaks up into two regions. The presence of disconnected instability regions has been reported also for optical bistability in a ring cavity [35]. A quantitative estimate of the errors introduced by truncation is obtained by tabulating for various N and several values of d the minimum values of C for which side-mode instabilities emerge in the $(x, \tau_\perp)$-plane (see table I). The

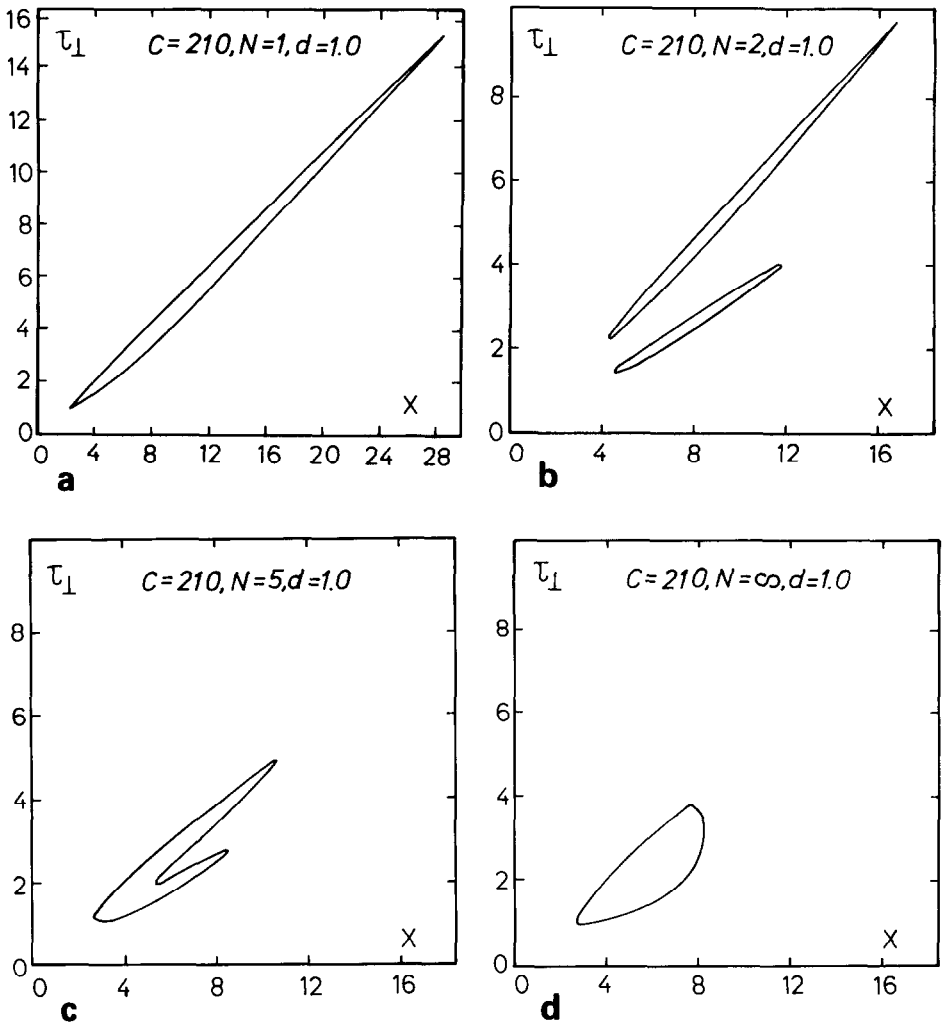

Fig. 2. Side-mode instability regions in the uniform-field limit as a function of the truncation parameter N.

convergence towards the physical case $N = \infty$ is found to be slow and oscillatory. Furthermore, the minimum values of C depend strongly on d. If we would redefine C and replace in (2.13) $\gamma_\perp$ by the geometric mean $(\gamma_\perp \gamma_\parallel)^{1/2}$, this dependence would be even more pronounced, so that it is not a trivial consequence of the scaling properties of C.

The values given in table I suggest that for fixed N and C the side-mode instability regions will enlarge, if d is augmented. Indeed, this conclusion is corroborated by numerical work; however, for increasing d the side-mode

Table I
Values for the cooperation parameter C, which correspond to the onset of side-mode instabilities in the $(x, \tau_\perp)$-plane, for various N and d. To calculate these values uniform-field theory has been employed.

N	1	2	3	5	10	∞
$d=0.5$	116.9	206.8	188.7	224.1	243.8	233.6
$d=1$	57.01	128.9	85.89	100.6	97.54	96.93
$d=2$	36.00	64.29	52.24	52.09	49.17	49.12

instability domain grows mainly in the direction of the $\tau_\perp$-axis. As it was already found [16] that for $d=1$ and $N=\infty$ side-mode instabilities can only be present in the negative-slope part of the steady-state curve $y(x)$, the occurrence of so-called positive-slope instabilities for $d \neq 1$ and infinite N is thus not likely. We verify this conjecture for the upper transmission branch of the bistability curve first. Here stability is guaranteed if we have

$$\operatorname{Re} \tilde{\lambda}_n^{(1)(\infty)} \leqslant \operatorname{Re} \tilde{\lambda}_0^{(1)(\infty)}, \tag{4.11}$$

along the upper transmission branch. According to (4.9) the left-hand side of this equation can be written as

$$\operatorname{Re} \tilde{\lambda}_n^{(1)(\infty)} = -\frac{1}{2} - \frac{C}{(1+\alpha^2)U} + \frac{C}{4x^2}\left[\frac{2+\alpha^2}{1+\alpha^2} - \frac{d_2 \operatorname{Re} U_\lambda}{d_1|U_\lambda|^2} + \frac{d_3 \operatorname{Im} U_\lambda}{d_1 \alpha |U_\lambda|^2} - \frac{d_4}{d_1(1+\alpha^2)U}\right], \tag{4.12}$$

with the definitions $\alpha = \pi\tau_\perp$, $d_1 = (d+1)^2 + \alpha^2$, $d_2 = d^2 + d + \alpha^2 + 2$, $d_3 = 2d^2 + 2d + \alpha^2$ and $d_4 = d^2 + d\alpha^2 + 3d$. Insertion of (4.7) and (4.12) in the above inequality gives

$$\frac{U^2(U^2-5) + \alpha^2 U^2(U-4) + 2(1+\alpha^2)}{(1+\alpha^2)U^3} + \frac{d_2 \operatorname{Re} U_\lambda}{d_1|U_\lambda|^2} + \frac{2d_3 d(d+1)x^2}{d_1 d_5 |U_\lambda|^2 \operatorname{Re} U_\lambda} + \frac{d_4}{d_1(1+\alpha^2)U} \geqslant 0, \tag{4.13}$$

with $d_5 = (d^2 + \alpha^2)(1+\alpha^2)$. It is clear that this statement is true for $U \geqslant 4$ or $x \geqslant \frac{1}{2}\sqrt{15}$, since $\operatorname{Re} U_\lambda > 0$. Hence, as long as the x-coordinate of the upper turning-point of the stationary curve exceeds $\frac{1}{2}\sqrt{15}$, the upper transmission branch of this curve remains stable. However, from the uniform-field steady-

Table II
The maximum x-values for side-mode instabilities at $C = 210$ for $d = 0.5$, 1 and 2 as a function of the truncation parameter N. For $d = 0.5$ and $N = 4, 8, \infty$ side-mode instabilities are not present. The bottom line displays the x-coordinates of the upper turning-point (utp) of the steady-state curve.

N	1	2	3	4	8	∞
$d = 0.5$	24.31	11.18	9.890	–	–	–
$d = 1$	28.61	16.78	13.74	11.43	9.023	8.290
$d = 2$	27.90	16.54	14.13	11.72	9.691	8.966
$x_{(\mathrm{utp})}$	11.78	12.90	13.33	13.57	13.90	13.97

state curve, namely $y = x + 4Cx/[U(U+1)]$, we infer that this requirement is fulfilled for $C \geq \frac{80}{11}$. This amount is well below the threshold $C = 49.12$ for side-mode instabilities (see table I). The lower transmission branch corresponds to values of x less than 0.653, for C above 49.12. So instabilities are not present in this branch either, if the inequality $\mathrm{Re}\,\tilde{\lambda}_n^{(1)(\infty)} < 0$ is satisfied for $0 \leq x \leq 0.653$. We have checked this requirement to be fulfilled.

The above results imply that the positive-slope instabilities for $N = 1$, found in ref. [11], are entirely accounted for by the truncation of the Bloch hierarchy. This can be illustrated by calculating, as a function of the truncation parameter N, the maximum x-values for side-mode instabilities and the x-coordinates of the upper turning-point for the bistability curve. From table II we see that the convergence of the former values is by far the slowest. Furthermore, it appears that for $N > 3$ positive-slope instabilities do not exist. This observation and the other findings of this section lead us to the conclusion that a study of the side-mode instabilities for the general set (3.24) is reliable only if one refrains from a truncation of the Bloch hierarchy.

Appendix

Evaluation of the matrix elements $H_{ij}^{(\pm)}$

In this appendix we firstly derive the expressions (3.25) and (3.26) for the matrix elements occurring in the differential equations (3.24) for the amplitude deviations of the electric field envelopes. Subsequently, we shall prove the relations (3.29) and (3.30) for the matrix elements that determine the phase deviations of the field envelopes.

The results (3.16) with (3.22) and (3.23) can be employed to obtain the inversion deviations $\Delta^{(+)}D_0$ and $\Delta^{(+)}D_1$ in terms of the stationary envelope fields and the deviations of the electric fields. With the use of (3.8) for $m = 1$

we then arrive at

$$\Delta^{(+)}P'_{\mathrm{F},1} = \sum_{i=1,2}\Big(-\frac{1+\lambda_\perp^{-1}}{2f}\{[e_iD_0+\bar{e}_iD_1][1+(1-4f_\lambda^2+4b_\lambda^2)D_{\lambda,0}] + [1-4f_\lambda^2+4b_\lambda^2]S_i^{(+)} + [1-4f_\lambda^2+4b_\lambda^2][e_iD_N+\bar{e}_iD_{N-1}]D_{\lambda,N}\} + \lambda_\perp^{-1}D_{i-1}\Big)\Delta^{(+)}e_i\,, \tag{A.1}$$

where we employed the short-hand notations $f = e_1 = \bar{e}_2$, $b = e_2 = \bar{e}_1$ and used the identity

$$D_1 = -\frac{(1+4f^2+4b^2)D_0+1}{8fb}\,, \tag{A.2}$$

which follows from (2.27). Furthermore, we introduce the sum

$$S_i^{(+)} = \sum_{j=1}^{N-1}(2e_iD_j+\bar{e}_iD_{j-1}+\bar{e}_iD_{j+1})D_{\lambda,j}\,, \tag{A.3}$$

for $i = 1, 2$. This sum can be evaluated by transforming it in several alternative ways and using the symmetry properties of the resulting equalities. The expression between the brackets at the right-hand side of (A.3) is proportional to D_j, since one has

$$D_j = -\frac{4fb}{1+4f^2+4b^2}(D_{j-1}+D_{j+1})\,, \tag{A.4}$$

with $j = 1, 2, 3, \ldots, N-1$. This can be established with the help of the explicit formulas (2.27) with (2.24). As a consequence the sum (A.3) for $i = 1$ turns out to be equal to

$$S_1^{(+)} = -\frac{1-4f^2+4b^2}{4f}\sum_{j=1}^{N-1}D_jD_{\lambda,j}\,. \tag{A.5}$$

On the other hand, a simple rearrangement of terms in (A.3) yields

$$S_1^{(+)} = 2f\sum_{j=1}^{N-1}D_jD_{\lambda,j} + b\sum_{j=1}^{N-1}(D_{j-1}D_{\lambda,j}+D_jD_{\lambda,j-1}) - b(D_1D_{\lambda,0}-D_ND_{\lambda,N-1})\,. \tag{A.6}$$

The sums at the right-hand sides of (A.5) and (A.6) are symmetric under the

simultaneous interchanges $f \leftrightarrow f_\lambda$ and $b \leftrightarrow b_\lambda$. Hence, upon equating these right-hand sides we may deduce two independent equalities, from which each of the sums may be solved. Substituting the results in (A.5) or (A.6) we find an expression for $S_1^{(+)}$,

$$S_1^{(+)} = \frac{b(1-4f^2+4b^2)}{\lambda_p - 1}\,(D_1 D_{\lambda,0} - D_0 D_{\lambda,1} + D_{N-1} D_{\lambda,N} - D_N D_{\lambda,N-1})\,. \tag{A.7}$$

An analogous expression for $S_2^{(+)}$ follows from the symmetry relation

$$S_2^{(+)}(f,b) = S_1^{(+)}(b,f)\,. \tag{A.8}$$

Substitution of these formulas in (A.1) provides us with the result

$$\begin{aligned}\Delta^{(+)}P'_{F,1} = &\left\{\frac{1+\lambda_\perp^{-1}}{16f^2}\left[1 + \frac{(1-4f^2+4b^2)^2}{1-\lambda_p} D_0 + \frac{(1-4f_\lambda^2+4b_\lambda^2)^2}{1-\lambda_p^{-1}} D_{\lambda,0}\right.\right.\\ &\left.\left. + 4(1-4f_\lambda^2+4b_\lambda^2)(f^2-b^2) D_N D_{\lambda,N}\right] + \lambda_\perp^{-1} D_0\right\}\Delta^{(+)}f\\ &+ \left\{\frac{1+\lambda_\perp^{-1}}{16fb}\left[1 + \frac{1-(4f^2-4b^2)^2}{1-\lambda_p} D_0 + \frac{1-(4f_\lambda^2-4b_\lambda^2)^2}{1-\lambda_p^{-1}} D_{\lambda,0}\right.\right.\\ &\left.\left. - 4(1-4f_\lambda^2+4b_\lambda^2)(f^2-b^2) D_N D_{\lambda,N}\right] + \lambda_\perp^{-1} D_1\right\}\Delta^{(+)}b\,. \end{aligned} \tag{A.9}$$

Here we made use of the identities (A.2) and

$$D_{N-1} = -\frac{1+2f^2+2b^2}{4fb} D_N\,, \tag{A.10}$$

which can be derived from (2.27). In view of (3.6) and (3.7) the proof of (3.25) and (3.26) is complete now.

From inspection of the system (3.6)–(3.11) it is obvious that the same method of solving these equations can be adopted for both the plus and the minus set. In order to verify the relations (3.29) and (3.30) for the matrix elements $H_{ij}^{(-)}$ we eliminate as before the polarization envelope deviations from the set (3.8)–(3.11). In this way we find a matrix equation for the N-dimensional vector $\{\Delta^{(-)}D_j\}$,

$$\lambda_p \sum_{j=1}^{N} \bar{M}_{(\lambda,N)i,j}\Delta^{(-)}D_j = F_i^{(-)}\Delta^{(-)}f + B_i^{(-)}\Delta^{(-)}b\,, \tag{A.11}$$

with $i = 1, 2, 3, \ldots, N$. The vectors $\boldsymbol{F}^{(-)}$ and $\boldsymbol{B}^{(-)}$ only depend on the stationary fields, as is shown by the formulas

$$F_i^{(-)} = 2(1 + \lambda_\perp) b (D_{i+1} - D_{i-1}) , \tag{A.12}$$

$$F_N^{(-)} = 2(1 - \lambda_\perp) f D_N - 2(1 + \lambda_\perp) b D_{N-1} , \tag{A.13}$$

for $i = 1, 2, 3, \ldots, N-1$, and the symmetry relation

$$B_i^{(-)}(f, b) = -F_i^{(-)}(b, f) , \tag{A.14}$$

valid for $i = 1, \ldots, N$. Inversion of the matrix $\bar{\mathbf{M}}_{\lambda,N}$, defined in section 2, shows that

$$[\bar{\mathbf{M}}^{-1}_{(\lambda,N)}]_{1,i} = -\frac{D_{\lambda,i}}{4 f_\lambda b_\lambda D_{\lambda,0}} , \tag{A.15}$$

for $i = 1, 2, 3, \ldots, N$. As a consequence the polarization deviation $\Delta^{(-)} P'_{\mathrm{F},1}$ is found to equal

$$\Delta^{(-)} P'_{\mathrm{F},1} = \sum_{i=1,2} \left\{ \lambda_\perp^{-1} D_{i-1} - \frac{(-1)^i (1 + \lambda_\perp^{-1}) \bar{e}_i}{2 f D_{\lambda,0}} (S^{(-)} + D_{N-1} D_{\lambda,N}) \right.$$
$$\left. - \frac{(-1)^i (1 - \lambda_\perp^{-1}) e_i}{2 f D_{\lambda,0}} D_N D_{\lambda,N} \right\} \Delta^{(-)} e_i . \tag{A.16}$$

The sum $S^{(-)}$ is given by

$$S^{(-)} = \sum_{j=1}^{N-1} (D_{j-1} - D_{j+1}) D_{\lambda,j} . \tag{A.17}$$

This sum can be reduced to a simpler expression in a similar fashion as demonstrated above for the sum $S_1^{(+)}$. If we write down (A.4) for the fields f_λ and b_λ and substitute the result in (A.17) we get

$$S^{(-)} = \frac{4 f_\lambda b_\lambda}{1 + 4 f_\lambda^2 + 4 b_\lambda^2} \left\{ \sum_{j=1}^{N-1} (D_{j+1} D_{\lambda,j-1} - D_{j-1} D_{\lambda,j+1}) - D_0 D_{\lambda,0} - D_1 D_{\lambda,1} \right.$$
$$\left. + D_{N-1} D_{\lambda,N-1} + D_N D_{\lambda,N} \right\} . \tag{A.18}$$

On the other hand a shift of indices in (A.17) leads to

$$S^{(-)} = \sum_{j=1}^{N-1} (D_{j-1} D_{\lambda,j} - D_j D_{\lambda,j-1}) + D_1 D_{\lambda,0} - D_N D_{\lambda,N-1} . \tag{A.19}$$

The sums in the right-hand sides of (A.18) and (A.19) are both antisymmetric under the simultaneous interchanges $f \leftrightarrow f_\lambda$ and $b \leftrightarrow b_\lambda$. Hence, equating these right-hand sides we may derive two equalities, as before. Solving these we get from (A.18) or (A.19)

$$S^{(-)} = \frac{8fb}{1-\lambda_p}\,(D_0 D_{\lambda,0} + D_1 D_{\lambda,1} - D_{N-1} D_{\lambda,N-1} - D_N D_{\lambda,N}) + \frac{(1+4f^2+4b^2)}{1-\lambda_p}\,(D_1 D_{\lambda,0} + D_0 D_{\lambda,1} - D_N D_{\lambda,N-1} - D_{N-1} D_{\lambda,N})\,. \tag{A.20}$$

With the use of this result and the relations (A.2), (A.10) the expression (A.16) can be recast in terms of the stationary fields D_0, $D_{\lambda,0}$, D_N and $D_{\lambda,N}$,

$$\Delta^{(-)} P'_{F,1} = \left\{ \frac{1+\lambda_\perp^{-1}}{16f^2}\,G + \frac{1}{2}\,(1-\lambda_\perp^{-1}) D_N D_{\lambda,N} D_{\lambda,0}^{-1} + \lambda_\perp^{-1} D_0 \right\} \Delta^{(-)} f + \left\{ -\frac{1+\lambda_\perp^{-1}}{16fb}\,G - \frac{1}{2}\,(1-\lambda_\perp^{-1})\,\frac{b}{f}\,D_N D_{\lambda,N} D_{\lambda,0}^{-1} + \lambda_\perp^{-1} D_1 \right\} \Delta^{(-)} b\,, \tag{A.21}$$

with G defined in (3.31). Insertion of this expression into (3.6) and comparison with (3.24) then yields the matrix elements $H_{11}^{(-)}$ and $H_{12}^{(-)}$ in the form given in (3.29) and (3.30). The other two matrix elements of (3.24) are trivially obtained from the symmetry relations (3.27) and (3.28).

References

[1] R. Bonifacio and L.A. Lugiato, Phys. Rev. A 18 (1978) 1129.
[2] R. Bonifacio and L.A. Lugiato, Lett. Nuovo Cim. 21 (1978) 505, 510.
[3] L.A. Lugiato, in: Progress in Optics XXI, E. Wolf, ed. (North-Holland, Amsterdam, 1984) p. 69.
[4] H.M. Gibbs, Optical Bistability: Controlling Light with Light (Academic Press, Orlando, FL, 1985).
[5] L.A. Lugiato, L.M. Narducci, J.R. Tredicce and D.K. Bandy, in: Instabilities and Chaos in Quantum Optics II, N.B. Abraham et al., eds. (Plenum, New York, 1988) p. 1.
[6] M. Gronchi, V. Benza, L.A. Lugiato, P. Meystre and M. Sargent III, Phys. Rev. A 24 (1981) 1419.
[7] H.J. Carmichael, R.R. Snapp and W.C. Schieve, Phys. Rev. A 26 (1982) 3408.
[8] H.J. Carmichael, Phys. Rev. A 28 (1983) 480.
[9] L.A. Lugiato, L.M. Narducci, E.V. Eschenazi, D.K. Bandy and N.B. Abraham, Phys. Rev. A 32 (1985) 1563.
[10] L.A. Lugiato, L.M. Narducci and M.F. Squicciarini, Phys. Rev. A 34 (1986) 3101.
[11] F. Casagrande, L.A. Lugiato and M.L. Asquini, Opt. Commun. 32 (1980) 492.

[12] M. Sargent III, Sov. J. Quantum Electron. 10 (1980) 1247.
[13] M.L. Asquini and F. Casagrande, Z. Phys. B 44 (1981) 233.
[14] H.J. Carmichael, J. Opt. Soc. Am. A 1 (1984) 1271.
[15] H.J. Carmichael, Opt. Commun. 53 (1985) 122.
[16] S. Maize, B.V. Thompson and S.S. Hassan, in: Optical Bistability III, H.M. Gibbs et al., eds. (Springer, Berlin, 1986) p. 352.
[17] I. Bar-Joseph and Y. Silberberg, Phys. Rev. A 36 (1987) 1731.
[18] H. Zeghlache, P. Mandel, N.B. Abraham, L.M. Hoffer, G.L. Lippi and T. Mello, Phys. Rev. A 37 (1988) 470.
[19] J.V. Moloney, M.R. Belic and H.M. Gibbs, Opt. Commun. 41 (1982) 379.
[20] J.V. Moloney, M. Sargent III and H.M. Gibbs, Opt. Commun. 44 (1983) 289.
[21] L.A. Lugiato, R.J. Horowicz, G. Strini and L.M. Narducci, Phil. Trans. R. Soc. London A 313 (1984) 291.
[22] L.A. Lugiato, F. Prati, L.M. Narducci, P. Ru, J.R. Tredicce and D.K. Bandy, Phys. Rev. A 37 (1988) 3847.
[23] L.A. Lugiato and L.M. Narducci, Z. Phys. B 71 (1988) 129.
[24] L.G. Suttorp and A.J. van Wonderen, in: Proc. European Quantum Electronics Conference 1988, Hannover, FRG, to be published; A.J. van Wonderen and L.G. Suttorp, to be published.
[25] J.A. Fleck, Jr., Appl. Phys. Lett. 13 (1968) 365.
[26] G.P. Agrawal and M. Lax, J. Opt. Soc. Am. 69 (1979) 1717.
[27] H.J. Carmichael and G.P. Agrawal, Opt. Commun. 34 (1980) 293.
[28] H.J. Carmichael and G.P. Agrawal, in: Optical Bistability I, C.M. Bowden et al., eds. (Plenum, New York, 1981) p. 237.
[29] W. Magnus, F. Oberhettinger and R.P. Soni, Formulas and Theorems for the Special Functions of Mathematical Physics (Springer, Berlin, 1966).
[30] R. Roy and M.S. Zubairy, Opt. Commun. 32 (1980) 163.
[31] J.A. Hermann, Opt. Acta 27 (1980) 159.
[32] H.J. Carmichael, Opt. Acta 27 (1980) 147.
[33] H.J. Carmichael, Phil. Trans. R. Soc. London A 313 (1984) 433.
[34] A.J. van Wonderen and L.G. Suttorp, to be published.
[35] M.L. Asquini, L.A. Lugiato, H.J. Carmichael and L.M. Narducci, Phys. Rev. A 33 (1986) 360.